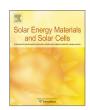
ELSEVIER

Contents lists available at ScienceDirect

Solar Energy Materials & Solar Cells

journal homepage: www.elsevier.com/locate/solmat



Atomic layer deposited zinc oxysulfide n-type buffer layers for Cu_2ZnSn (S,Se)₄ thin film solar cells



Hee Kyeung Hong ^a, In Young Kim ^a, Seung Wook Shin ^b, Gwang Yeom Song ^a, Jae Yu Cho ^a, Myeng Gil Gang ^a, Jae Cheol Shin ^c, Jin Hyeok Kim ^a, Jaeyeong Heo ^{a,*}

- ^a Department of Materials Science and Engineering, and Optoelectronics Convergence Research Center, Chonnam National University, Gwangju 61186, Republic of Korea
- b Department of Chemical Engineering and Materials Science, University of Minnesota, Minneapolis, MN 55455, USA
- ^c Department of Physics, Yeungnam University, Gyeongsan 38541, Republic of Korea

ARTICLE INFO

Article history:
Received 26 December 2015
Received in revised form
8 April 2016
Accepted 29 April 2016
Available online 14 May 2016

Keywords: Cu₂ZnSn(S,Se)₄ Buffer layer Zn(O,S) Atomic layer deposition Efficiency

ABSTRACT

The structural, electrical, chemical, and optical properties of ternary Zn(O,S) thin films formed by atomic layer deposition (ALD) were investigated. It was revealed that the film's characteristics were highly influenced by the O/(O+S) ratio. The n-type Zn(O,S) layer was applied to both S-rich and Se-rich Cu₂ZnSn (S,Se)₄ (CZTSSe) absorbers as an alternative buffer layer to conventional CdS. The device performance relationship to the O/(O+S) ratio was examined. The highest power-conversion efficiency (PCE) of 2.75% and 3.30% was achieved using an actual O/(O+S) ratio of \sim 0.67 in the buffer layer for S-rich and Se-rich CZTSSe solar cells, and these PCEs correspond to 77% and 67% of the standard CdS-based solar cells, respectively. Further improvement in Se-rich CZTSSe was demonstrated by using NH₄OH solution instead of pure H₂O as oxygen source during ALD process. The dependence of the solar cell performance on the O/(O+S) ratio was investigated using dark current density–voltage (J–V), external quantum efficiency (EQE), transmission electron microscopy (TEM), and energy-dispersive X-ray spectroscopy (EDX).

© 2016 Elsevier B.V. All rights reserved.

1. Introduction

Wide bandgap materials have been used for various applications including solar cell devices, flat panel displays, and light-emitting diodes [1,2]. Thin film solar cells (TFSCs) are one of the applications in which wide bandgap materials, i. e., zinc oxide (ZnO) or indium-tin-oxide (ITO), are used as window layers [3]. The representative TFSC absorber material is Cu(In,Ga)Se₂ (CIGS), and a maximum power-conversion efficiency (PCE) of \sim 21% was recently reported [4]. There are several factors affecting the PCE of TFSCs, and the conduction band offset and the interface quality between an absorber layer and an n-type buffer layer are among them [5,6]. In addition, intrinsic characteristics of an n-type buffer layer also influence the overall PCE of TFSCs [7].

Various n-type buffer layers were used to remove detrimental defects between a p-type absorber and a highly doped n-type window layer. CdS is one of the most researched buffer materials [8,9], which is generally deposited by a chemical bath deposition (CBD) method. Due to the toxicity of Cd and its low bandgap (~ 2.4 eV), many studies have attempted to replace CdS with Cd-

free buffer layers. ZnO-based buffer layers have been intensively studied because of their high bandgap of \sim 3.3 eV. In order to modulate and tune the band offset between the absorber and buffer layers, additional oxide or sulfide was added, producing ternary oxide (or oxysulfide). (Zn,Sn)O [10–12], (Zn,Mg)O [13,14], and Zn(O,S) [15] are the representative buffer layers. Zn(O,S) has been highlighted as a strong candidate for an n-type buffer layer because its band offset can be easily tuned by varying the oxygen-to-sulfur ratio [16,17]. This tuning can be enacted by using atomic layer deposition (ALD), alternately controlling layers of ZnO and ZnS growth [18]. ALD is suitable for solar cell applications because of its excellent conformality and composition control. ALD-Zn(O,S) buffer layers have also been applied to SnS [19] and Cu₂O [20] TFSCs, but most studies have focused on the performance enhancement of CIGS-based solar cells [15,21–23].

Recently, research has rapidly expanded on fabricating earth-abundant solar cells that can possibly replace CIGS-based cells. One of the candidate materials is Cu₂ZnSn(S,Se)₄ (CZTSSe) [24–28]. A detailed and comparative study of ALD-based buffer layers on CZTSSe TFSCs is crucial to improve the PCE. However, relatively little work has been reported on how ALD-Zn(O,S) buffer layers influence the PCE of CZTSSe TFSCs [29]. Sputter-(Zn,Mg)O layers have been investigated as alternative buffer layers, but the sputter

^{*} Correspondence to: 77 Yongbong-ro, Buk-gu, Gwangju 61186, Republic of Korea. E-mail address: jheo@jnu.ac.kr (J. Heo).

damage on a CZTSSe layer seriously degraded the cell performance [30]. In this regard, application of ALD-buffer layers on CZTSSe solar cells may be advantageous considering the damage-free growth mechanism and fine stoichiometric control offered by ALD growth. When ternary materials are formed by ALD, however, the growth behaviors differ from those that would be expected based on the linear combinations of its binary components, and therefore, care should be taken for each ALD multicomponent growth process [4,31-33]. Also, chemical interaction during the pulse of the precursor and reactant with the absorber is important to determine the junction quality [34]. While varying the O/(O+S)ratio, the structural, electrical, chemical, and optical properties of Zn(O,S) thin films were studied in detail. Finally, the Zn(O,S) thin films were applied as n-type buffer layers for S-rich and Se-rich CZTSSe TFSCs, and their performance was compared with the control CdS-buffer-based cells. Further improvement in PCE was demonstrated by replacing H₂O with 27 wt% NH₄OH solution as oxygen source during ALD-Zn(O,S).

2. Experimental

Zn(O,S) thin films were formed by using a laminar-flow thermal ALD reactor (NCD, Lucida D100, Korea). Diethylzinc (DEZ, EGChem., Korea), deionized water (H₂O), and 10% hydrogen sulfide (H₂S mixed with N₂, Gaschem., Korea) were used as Zn, O, and S sources, respectively. The ZnO growth cycle consisted of a DEZ pulse (0.2 s), N_2 purge (10 s), H_2O pulse (0.2 s), and N_2 purge (20 s). The ZnS growth cycle consisted of a DEZ pulse (0.2 s), N2 purge (10 s), H₂S pulse (5 s), and N₂ purge (10 s). Zn(O,S) thin films with different O/(O+S) ratios were deposited by controlling subcycle numbers of ZnO (m) and ZnS (n). For general property examination, the combination of m:n was controlled from 32:1 (O-rich) to 1:4 (S-rich) as well as 1:0 (pure ZnO) and 0:1 (pure ZnS). Combinations of m:n including 4:1, 6:1, 7:1, 8:1, 9:1, 11:1, 16:1, 32:1 and 1:0 were applied for solar cell fabrication. These conditions were chosen based on the preliminary examination of the effect of the *m*:*n* ratio on the PCE of the cells; O-rich Zn(O,S) buffer layers led to higher PCE, as discussed later. For further improvement in PCE, we later used NH₄OH solution (Sigma Aldrich, 27 wt%) instead of pure H₂O as O source during ZnO subcycle. The pulse and purge time was maintained like the normal ZnO process using H₂O. If not mentioned otherwise, the results are obtained from H₂O-based ALD-Zn(O,S) process. ALD growth temperature was set at 120 °C based on the ALD-ZnO growth temperature window. Zn(O,S) formation using dimethylzinc was reported by Bakke et al. [35], and detailed ALD metal sulfide film growth was recently reviewed [36,37]. The thickness of the Zn(O,S) films was set to be \sim 50 nm for property analyses.

CZT metal layers were deposited on Mo/glass substrates by using a dc sputtering system (SNTEK, Korea). Pure Zn, Sn, and Cu metals were sequentially sputtered at 8 mTorr pressure with a dc power of 30 W at room temperature. Then, the metal layers were rapid-thermal-annealed (RTA) at 520 °C for 10 min (Ajeon, Korea) under ambient Ar preloaded with S (0.0075 g)/Se (0.03 g) powder. The prepared S-rich Cu₂Zn_{1.4}Sn_{1.2}S_{4.4}Se_{0.8} absorber layers were vacuum-sealed prior to the formation of buffer layers. Se-rich CZTSSe absorber layers (Cu_{1.8}Zn₂Sn_{1.4}S_{1.4}Se_{3.4}) were also prepared in the similar manner, but with different amount of S (0.003 g)/Se (0.077 g) powder during RTA. Here, the composition of the CZTSSe absorber layers on Mo/glass substrates was estimated from wavelength-dispersive X-ray fluorescence (XRF, Rigaku, ZSX Primus II). More details on the sample fabrication and measurements can be found elsewhere [38,39]. The final absorber thickness was $\sim\!0.8\text{--}1.1\,\mu\text{m}.$ The absorber was KCN etched for 5 min. Then, the samples were immediately transferred to the ALD chamber and

buffer layers with various O/(O+S) ratios were grown. The target buffer thickness was $100 \, \mathrm{nm} \ (\pm 5 \, \mathrm{nm})$. Sequentially conducting ALD-ZnO with a thickness of $\sim 30 \, \mathrm{nm}$ was deposited as an antisputter damage layer. A conventional CBD-CdS buffer layer of $\sim 70 \, \mathrm{nm}$ was also formed on some of the CZTSSe absorbers for comparison. Detailed CdS growth conditions are reported elsewhere [40]. After the formation of the buffer layer, intrinsic-ZnO, Al-doped ZnO layers, and Al metal grids were deposited by using rf and dc sputtering systems. Cell isolation was achieved by mechanical scribing, and a bottom Mo electrode was connected using silver paste for electrical contact. Each cell was $0.31 \, \mathrm{cm}^2$, and six cells were fabricated from one sample.

The film thickness and refractive index of the Zn(O.S) films were measured using an ellipsometer (Gaertner, Stokes Ellipsometer LSE). The crystallinity of the Zn(O,S) films was examined by glancing angle X-ray diffraction (GAXRD, PANalytical, X'Pert Pro MPD) at $\omega = 1^{\circ}$ and high-resolution transmission electron microscopy (HR-TEM, JEOL, JEM-2100F) operating at 200 kV. X-ray photoelectron spectroscopy (XPS, VG, Multilab 2000) analysis was used for estimating the actual composition of the grown Zn(O, S) films. Surface morphologies were investigated by using atomic force microscopy (AFM, Park systems, XE100). The electrical properties of the grown films were obtained by Hall measurements (Ecopia, HMS-3000) using a Van der Pauw configuration and a four-point probe (Changmin Tech., CMT-SR2000). The optical properties were analyzed by using an ultraviolet-visible spectrophotometer (Agilent, Cary 5000), and the estimation of the optical bandgaps was performed.

The current density–voltage characteristics (J-V) of the solar cell devices under illumination and dark conditions were measured using Keithley 2400 and Keithley 236 SourceMeter systems, respectively. The standard 1-sun illumination was generated by a solar simulator (San-ei Electric, XES-301S). External quantum efficiency (EQE) of the fabricated solar cells was analyzed by using a spectral response measurement system (Jasco, CEP-25BX). For structural and elemental analyses of the fabricated devices, analytical scanning TEM (STEM, JEOL, 2100F) operated at 200 kV was used. TEM samples were prepared using a FEI Nova 600 Nanolab focused ion beam.

3. Results and discussion

Fig. 1 shows the change in the average growth-*per*-cycle (GPC) depending on the ZnO cycle ratio, defined as m/(m+n), at 120 °C grown on Si substrate. The average GPCs of pure ZnS and ZnO were ~ 0.137 and ~ 0.147 nm cycle $^{-1}$, respectively. As the ZnO cycle ratio approaches 0.8, GPC decreases compared to the pure ZnO and ZnS cases, which may be due to the delayed nucleation of ZnO and ZnS on heterogeneous ZnS and ZnO surfaces, respectively. Similar decreases in GPC for the mixed cycle ratio are observed for (Zn,Sn) O [10] and (Zn,Al)O [4]. Refractive indices of the Zn(O,S) films at ~ 50 nm thickness also decreased from ~ 2.3 for pure ZnS to ~ 1.9 for pure ZnO. Both GPC and refractive index drastically changed starting at a ZnO cycle ratio of 0.8.

Fig. 2 shows the glancing angle X-ray diffraction results of Zn(O, S) films grown on glass substrates with various ZnO cycle ratios. Both pure ZnO and ZnS films exhibit hexagonal wurtzite structures (JCPDS 00-036-1451 and 00-036-1450, respectively). When a small number of ZnO cycles are added to ZnS, the peak intensity of ZnS h (002) decreases, and the peak position shifts to a higher angle. When the ZnO cycle ratio is 0.8 (m:n=4:1), the lowest peak intensity is obtained. The grain size calculated from the Scherrer formula yielded an average size of $\sim 14-18$ nm for all films, except for the film with a ZnO cycle ratio of 0.8, with a grain size of ~ 5 nm. As the ZnO cycle increases beyond 4:1, amorphous phases

Download English Version:

https://daneshyari.com/en/article/77488

Download Persian Version:

https://daneshyari.com/article/77488

<u>Daneshyari.com</u>